HHS Public Access

Author manuscript

Oncogene. Author manuscript; available in PMC 2016 January 01.

Published in final edited form as:

Oncogene. 2015 July ; 34(29): 3760–3769. doi:10.1038/onc.2014.292.

Anticipatory Estrogen Activation of the Unfolded Protein Response is Linked to Cell Proliferation and Poor Survival in Estrogen Receptor α Positive Breast Cancer

Neal Andruska[1,4], **Xiaobin Zheng**[1], **Xujuan Yang**[2], **William G. Helferich**[2,3,4], and **David J. Shapiro**[1,3,4]

[1]Department of Biochemistry, University of Illinois, Urbana, IL, 61801, USA

[2]Department of Food Science & Human Nutrition, University of Illinois, Urbana, IL, 61801, USA

[3]University of Illinois Cancer Center, University of Illinois

[4]College of Medicine, University of Illinois

Abstract

In response to cell stress, cancer cells often activate the endoplasmic reticulum (EnR) stress sensor, the unfolded protein response (UPR). Little was known about the potential role in cancer of a different mode of UPR activation; anticipatory activation of the UPR prior to accumulation of unfolded protein or cell stress. We show that estrogen, acting via estrogen receptor α (ERα), induces rapid anticipatory activation of the UPR, resulting in increased production of the antiapoptotic chaperone BiP/GRP78, preparing cancer cells for the increased protein production required for subsequent estrogen-ERα induced cell proliferation. In ERα containing cancer cells, the estrogen, 17β-estradiol (E_2) activates the UPR through a phospholipase C γ (PLCγ)-mediated opening of EnR IP_3R calcium channels, enabling passage of calcium from the lumen of the EnR into the cytosol. siRNA knockdown of ERα blocked the estrogen-mediated increase in cytosol calcium and UPR activation. Knockdown or inhibition of PLCγ, or of IP_3R, strongly inhibited the estrogen-mediated increases in cytosol calcium, UPR activation and cell proliferation. E_2-ERα activates all three arms of the UPR in breast and ovarian cancer cells in culture and in a mouse xenograft. Knockdown of ATF6α, which regulates UPR chaperones, blocked estrogen induction of BiP and strongly inhibited E_2-ERα stimulated cell proliferation. Mild and transient UPR activation by estrogen promotes an adaptive UPR response that protects cells against subsequent UPR-mediated apoptosis. Analysis of data from ERα positive breast cancers demonstrates elevated expression of a UPR gene signature that is a powerful new prognostic marker tightly correlated with subsequent resistance to tamoxifen therapy, reduced time to recurrence and poor survival. Thus, as an early component of the E_2-ERα proliferation program, the mitogen estrogen,

Correspondence: Dave Shapiro; University of Illinois, 419 Roger Adams Lab, 600 S. Mathews Avenue, Urbana, IL 61801; 217-333-1788; djshapir@illinois.edu.

CONFLICTS OF INTEREST

The authors declare no conflicts of interest.

Supplementary Information accompanies the paper on the *Oncogene* website (http://www.nature.com/onc).

drives rapid anticipatory activation of the UPR. Anticipatory activation of the UPR is a new role for estrogens in cancer cell proliferation and resistance to therapy.

Keywords

Estrogen receptor α; breast cancer; ovarian cancer; unfolded protein response (UPR)

INTRODUCTION

Estrogens, acting via estrogen receptor α (ERα), stimulate cell proliferation and tumor growth.[1–3] The importance of estrogens and ERα in breast cancer is illustrated by the central role of endocrine therapy targeting estrogens and ERα in treatment of ERα$^+$ breast cancer.[1–5] To help fold and sort the increased protein required for estrogen-ERα induced cell proliferation, cells must increase chaperone levels. The endoplasmic reticulum (EnR) stress sensor, the unfolded protein response (UPR) monitors and maintains protein-folding homeostasis.[6, 7] The UPR responds to misfolded proteins, or other forms of stress, by activating three signal transduction pathways, which reduce protein production and increase EnR protein-folding capacity. Protein production is regulated by autophosphorylation of the stress-activated transmembrane kinase, PERK.[6, 7] P-PERK phosphorylates eukaryotic initiation factor 2α (eIF2α), resulting in transient inhibition of protein synthesis. The other UPR arms initiate with proteolytic activation of the transcription factor ATF6α, leading to increased chaperone production and activation of the EnR splicing factor IRE1α, which alternatively splices the transcription factor XBP1, leading to production of active spliced-XBP1, increased protein folding capacity and altered mRNA decay and translation.[6, 7]

The UPR is usually inactive in normal cells, but is overexpressed in several cancers.[8] Chronic UPR activation leads to increased expression of EnR chaperones, such as BiP (GRP78/HSAP5), p58^{IPK} and calreticulin that facilitate protein folding and promote survival, proliferation, angiogenesis, and resistance to chemotherapy and endocrine therapy.[9–12] In the widely studied “reactive mode”, the UPR in tumor cells is activated in response to accumulation of stress from rapid cell division, hypoxia and therapy. A few studies in immune cells describe a different type of UPR activation; in this “anticipatory mode”, the UPR is activated in the absence of EnR stress and prior to the accumulation of unfolded proteins.[13, 14] We explored whether estrogen induces anticipatory activation of the UPR in the absence of EnR stress, increasing protein folding capacity prior to the increased protein production and protein folding load that accompanies activation of the genomic estrogen-ERα cell proliferation program. Previous studies of the UPR and of estrogen-ERα action focused on the estrogen-inducible UPR gene, XBP1. XBP1 binds to and activates ERα; XBP1 expression is associated with tamoxifen resistance in ERα$^+$ breast cancer.[15–18]

The plasma membrane enzyme phospholipase C γ (PLCγ) hydrolyzes PIP_2 to diacyglycerol (DAG) and inositol 1,4,5-triphosphate (IP_3). We show that the mitogen estrogen, 17β-estradiol (E_2), acting through a rapid extranuclear action of ERα, elicits a PLCγ-mediated opening of EnR IP_3R calcium channels, increasing cytosol calcium and triggering anticipatory activation of each arm of the UPR. Opening the IP_3R calcium channel and

activating the ATF6α arm of the UPR, resulting in BiP induction, are important for subsequent E_2-ERα induced cell proliferation. Consistent with an important role in cancer for anticipatory activation of the UPR, analysis of data from ~1,000 ERα$^+$ breast cancer patients demonstrates that elevated expression of a UPR gene signature is tightly correlated with subsequent resistance to tamoxifen therapy, time to tumor recurrence and poor survival.

RESULTS

Estrogen Activates all 3 Arms of the UPR

To evaluate the ability of E_2-ERα to activate the UPR, we focused on production of spliced and modified proteins that result from activating the three arms of the UPR (Supplementary Figure 1). E_2 rapidly activated the IRE1α arm of the UPR, as shown by increases in spliced-XBP1 (sp-XBP1) mRNA in T47D and MCF-7 breast and PEO4 ovarian cancer cells (Figure 1a and b), and by induction of downstream sp-XBP1 targets, SERP1 and ERDJ (Supplementary Figure 2a).[19] The antiestrogens ICI 182,780/Faslodex/fulvestrant (ICI) and 4-hydroxytamoxifen, (4-OHT), which compete with E_2 for binding to ERα, blocked the E_2-mediated increase in sp-XBP1 (Figure 1a). Consistent with E_2-ERα activating the IRE1α arm of the UPR, RNAi knockdown of ERα blocked E_2-induction of sp-XBP1 mRNA (Figure 1c), and induction of GREB1 by nuclear E_2-ERα (Supplementary Figure 2b).

We next assessed whether estrogen activates the ATF6α arm of the UPR. ATF6α is a 90 kDa protein (p90-ATF6α) that translocates from the EnR to the Golgi in response to stress, where it undergoes proteolytic cleavage to its active 50 kDa form (p50-ATF6α) (Supplementary Figure 1b).[6, 7, 20] Increased ATF6α proteolysis in T47D cells and PEO4 cells demonstrates that E_2-ERα transiently activates the ATF6α arm of the UPR (Figure 1d; Supplementary Figure 2c). Since pretreatment with ICI, abolished the E_2-mediated increase in p50-ATF6α, this effect is mediated through ERα (Figure 1d). Active cleaved ATF6α regulates induction of BiP and other EnR chaperones.[20, 21] Consistent with this, ATF6α knockdown in T47D cells blocked BiP induction (Figure 1e). BiP increases EnR protein folding capacity, contributing to resolution of the stress, and helps reverse UPR activation; likely preventing the cytotoxicity that would result if UPR activation was sustained. Consistent with its antiapoptotic role, in several cancers, elevated levels of BiP are associated with a poor prognosis.[9] Estrogen rapidly induced BiP mRNA in breast and ovarian cancer cells (Figure 1f), leading to a 2.3-fold increase in BiP protein (Figure 1g). RNAi knockdown of ERα prevented E_2-induction of BiP mRNA (Figure 1h).

PERK activation leads to inhibition of protein synthesis (Supplementary Figure 1c). Surprisingly, E_2 induces a rapid and transient increase in PERK phosphorylation (Figure 2a), resulting in increased phosphorylation of eIF2α (Figure 2b) and a modest transient decline in overall protein synthesis (Figure 2c). Consistent with p-PERK catalyzing formation of p-eIF2α, PERK knockdown inhibited formation of p-eIF2α (Figure 2d). Consistent with E_2 acting through ERα, ICI inhibited E_2-stimulated phosphorylation of PERK and eIF2α and largely reversed the E_2-mediated inhibition of protein synthesis (Figure 2a, b, and c). PERK activation leads to ATF4 expression, and we observed a transient increase in ATF4 expression (Figure 2e). However, the proapoptotic protein CHOP was not induced because mild and transient activation of PERK does not induce CHOP

(Figure 2f; Supplementary Figure 2d).[22] Together, this data demonstrates that E_2, acting through ERα, activates all three UPR arms.

E_2-ERα Rapidly Increases Cytosol Ca^{2+} by a PLCγ-mediated Opening of the EnR IP_3R Ca^{2+} Channel, Activating the UPR

Rapid UPR activation by E_2-ERα suggested accumulation of unfolded protein was not triggering UPR activation. Some UPR activators, such as thapsigargin, rapidly activate the UPR by depleting Ca^{2+} stores in the lumen of the EnR, increasing intracellular Ca^{2+}. To test whether E_2 rapidly alters cytosol Ca^{2+}, we monitored cytosol calcium using the sensor dye Fluo-4 AM. In the presence or absence of extracellular Ca^{2+}, estrogen produced a rapid and transient increase in fluorescence in T47D breast cancer cells (Figure 3a and b). Since E_2 increases cytosol Ca^{2+} when there is no extracellular Ca^{2+}, and the EnR lumen is the major Ca^{2+} store available to increase cytosol Ca^{2+}, E_2 is acting by depleting the EnR Ca^{2+} store. Estrogen also increased cytosol calcium in PEO4 ovarian cancer cells (Supplementary Figure 3). Inhibition of the IP_3R channel with 2-APB, which locks the IP_3R Ca^{2+} channels closed, and RNAi knockdown of the three isoforms of the IP_3R channels (Figure 3c), abolished the rapid E_2-ERα-mediated increase in cytosol Ca^{2+} (Figure 3a, b, and d). In contrast, high concentration ryanodine (Ry), which closes the ryanodine receptor (RyR) Ca^{2+} channels, did not block the increase in cytosol Ca^{2+} (Figure 3a and b). We next assessed whether Ca^{2+} release was necessary for UPR activation using 2-APB and ryanodine individually, or in combination. 2-APB, but not ryanodine, inhibited E_2-ERα activation of the PERK arm of the UPR, as shown by inhibition of formation of p-eIF2α (Supplementary Figure 4a). RNAi knockdown of IP_3R (Figure 3c) blocked E_2-induced Ca^{2+} release (Figure 3d), activation of the IRE1α arm of the UPR (Supplementary Figure 4b), and blocked E_2-induction of BiP (Figure 3c), which is a commonly used surrogate readout for UPR activation.

We next tested the possibility that activation of PLCγ, which hydrolyzes PIP_2 to DAG and IP_3, plays a role in E_2-mediated opening of the IP_3R Ca^{2+} channels. Treating T47D cells with the PLCγ inhibitor, U73122, or siRNA knockdown of PLCγ, abolished the rapid E_2-ERα-mediated increase in cytosol Ca^{2+} (Figure 3e and f; Supplementary Figure 5). Since PLCγ mediates E_2-dependent opening of the IP_3R Ca^{2+} channels and calcium release (Figure 3f), we examined the effect of siRNA knockdown of PLCγ on E_2-ERα-dependent activation of the UPR. siRNA knockdown of PLCγ blocked E_2-ERα activation of the ATF6α arm of the UPR, as shown by a reduction in p50-ATF6α, and inhibition of BiP induction (Figure 3e).

To evaluate the role of ERα in the E_2-mediated increase in cytosol calcium, we performed siRNA knockdown. In T47D cells, RNAi knockdown of ERα, in the absence of extracellular Ca^{2+}, prevented E_2-stimulated calcium release (Figure 3g and h; Supplementary Movie 1 and 2). PLCγ is on the inner leaflet of the plasma membrane and the E_2-ERα-mediated increase in cytosol Ca^{2+} occurs in <2 min. Thus, the E_2-ERα-mediated increase in intracellular Ca^{2+} that leads to UPR activation is a rapid, extranuclear action of ERα at the plasma membrane.

The UPR and E_2-ERα Action in E_2-ERα Stimulated Cell Proliferation

We explored the role of Ca^{2+} release from the EnR in promoting E_2-ERα induced gene expression, UPR activation, and subsequent cell proliferation. Consistent with a possible role for intracellular Ca^{2+} in E_2-ERα action,[23] chelating intracellular Ca^{2+} with BAPTA-AM blocked E_2-stimulated cell proliferation (Supplementary Figure 6a). In T47D cells, PLCγ or IP_3R knockdown, or locking IP_3R with 2-APB, strongly inhibited the increase in cytosol Ca^{2+} (Figure 3a, b, d, and f), UPR activation (Figure 3c and e; Supplementary Figure 4), and E_2-ERα-stimulated cell proliferation (Figure 4a and b). However, IP_3R knockdown did not inhibit E_2-dependent down-regulation of ERα or E_2-induction of GREB1 or pS2 mRNA (Figure 4c; Supplementary Figure 6b).[24, 25] Similarly, 2-APB did not abolish E_2-ERα induced expression of stably transfected ERE-luciferase in T47D cells, while 2-APB and Ry together, strongly inhibited reporter gene expression (Figure 4d). This suggests there are different intracellular Ca^{2+} requirements for E_2-ERα-mediated UPR activation and E_2-ERα-mediated gene expression. Importantly, the IP_3R knockdown data uncouples UPR activation from E_2-ERα-mediated gene expression, and demonstrates that blocking UPR activation is sufficient to inhibit estrogen-stimulated cell proliferation.

We next evaluated the role of E_2-induction of EnR chaperones in E_2-ERα-stimulated cell proliferation. Knockdown of PLCγ or IP_3R strongly inhibited E_2-induction of BiP and E_2-ERα-stimulated cell proliferation (Figures 3c, 3e, and 4a). Knockdown of the primary UPR regulator of EnR chaperones, ATF6α, also strongly inhibited E_2-induction of BiP and E_2-ERα-stimulated cell proliferation (Figure 1e and 4a). Thus, UPR activation and subsequent induction of EnR chaperones plays an important role in E_2-ERα-stimulated cell proliferation.

We further evaluated the effects of PLCγ, IP_3R, ATF6α, XBP1, and PERK knockdown on E_2-stimulated proliferation of MCF-7 cells (Supplementary Figure 7). Knockdown of the ATF6α and XBP1 arms of the UPR produced 40% declines in E_2-stimulated in cell proliferation, while PERK knockdown produced a 20% decline (Figure 4e). IP_3R knockdown produced a 50% decline in E_2-ERα-stimulated MCF-7 cell proliferation (Figure 4e). This is consistent with the 40% decline in proliferation following 2-APB treatment (Supplementary Figure 6c), which did not fully abolish E_2-induction of pS2 and GREB1 mRNA (Figure 4f; Supplementary Figure 6d). Targeting IP_3R in MCF-7 cells produced less dramatic inhibition of E_2-ERα-stimulated cell proliferation compared to T47D cells or BG-1 ovarian cancer cells (Figure 4a, b, and e; Supplementary Figure 6c and e). Knockdown of PLCγ in MCF-7 cells nearly abolished E_2-ERα-stimulated cell proliferation (Figure 4e). Together, this data demonstrates that weak anticipatory activation of the UPR, resulting in induction of chaperones, plays an important role in E_2-ERα-stimulated cell proliferation. This novel E_2-ERα pathway leading to cancer cell proliferation is shown (Figure 4g).

E_2-ERα Action Increases Levels of UPR Sensors and Downstream Targets

We investigated whether E_2-ERα facilitates UPR activation by inducing the sensors that trigger activation of the three UPR arms. E_2 rapidly induced mRNAs encoding sensors for all 3 UPR arms and the chaperones BiP and GRP94 (Figure 5a). These were early responses, usually visible within 2 hours. Although some responses declined at later times, estrogen

produced sustained increases in resident chaperones and some UPR components, such as eIF2α (Figure 5a).

E_2-ERα-regulated Gene Expression and UPR Activation are Correlated *In Vivo*

To assess *in vivo* relevance, we used growing MCF-7 tumors receiving estrogen and regressing MCF-7 tumors receiving only cholesterol vehicle (Figure 5b) and compared expression of classical measures of E_2-ERα activity to markers of UPR activation.[26] In the $+E_2$ tumors, the markers for E_2-ERα activity, pS2 and GREB1 mRNAs,[24, 25] were induced 12-fold and 17-fold and all three UPR arms were moderately activated (Figure 5c and d). Consistent with activation of the IRE1α arm of the UPR, sp-XBP1 increased 3-fold, while total XBP1 declined (Figure 5d). Consistent with E_2-activation of the ATF6α arm of the UPR, $+E_2$ tumors displayed 2.0 and 1.8-fold increases in BiP and GRP94 mRNAs, respectively (Figure 5d). Levels of CHOP and GADD34 mRNA were 2.1-fold and 1.4-fold higher in the $+E_2$ group, respectively, indicating weak activation of the PERK arm (Figure 5d). While levels of primary UPR sensors IRE1α and PERK were reduced in these tamoxifen-sensitive tumors, their immediate targets eIF2α and sp-XBP1 were increased (Figure 5d).

To assess UPR activity early in $ERα^+$ breast cancer development, we compared E_2-ERα activity and UPR pathway activity in samples of histologically normal breast epithelium and invasive ductal carcinoma (IDC). Compared to normal epithelium from IDC patients, IDC samples displayed elevated levels of ERα mRNA and E_2-ERα induced pS2 and GREB1 mRNAs, and reduced levels of E_2-ERα downregulated IL1-R1 mRNA (Figure 5e). IDC samples displayed elevated SERP1 mRNA, a marker for IRE1α activation;[19] CHOP and GADD34, which are markers of PERK activation; and BiP and GRP94 chaperones, which are markers of ATF6α activation (Figure 5f). These data suggest UPR activation occurs very early in tumor development.

Using data from an independent cohort of 278 $ERα^+$ breast cancers we explored whether expression of ERα mRNA and protein, or E_2-ERα-regulated genes, correlates with expression of UPR genes. Expression of several UPR genes displayed highly significant correlation with expression of ERα and ERα-target genes (Supplementary Table 1).

Prior Estrogen Activation of the UPR Protect Cells from Subsequent Exposure to Cell Stress

Weakly activating, non-toxic, concentrations of the UPR activator, tunicamcyin (TUN), elicit an adaptive stress response that increases EnR chaperones, and renders cells resistant to subsequent exposure to an otherwise lethal concentration of tunicamycin.[27, 22] Consistent with weak E_2 activation of the UPR, E_2 induces a 2.3-fold increase in BiP protein compared to a 5.5-fold increase in BiP following maximal UPR activation by a lethal concentration of tunicamycin (Figure 1g and Supplementary Figure 8). We tested whether prior exposure of T47D cells to E_2, or a low concentration of tunicamycin, altered the concentration of tunicamycin required to subsequently induce substantial cell death. Pre-treating cells with estrogen or TUN had nearly identical effects; each elicited an ~10 fold increase in the concentration of tunicamycin required to induce apoptosis (Figure 6a). Thus, the E_2-induced

weak anticipatory activation of the UPR both facilitates tumor cell proliferation and is a potential mechanism by which estrogen might protect ERα$^+$ breast tumors against subsequent apoptosis due to hypoxia, nutritional deprivation and therapy.

A UPR Gene Signature Predicts Clinical Outcome in ERαPositive Breast Cancer

To explore UPR activation as a potential prognostic marker in ERα$^+$ breast cancer, we developed a UPR gene signature consisting of genes encoding components of the UPR pathway and downstream targets of UPR activation (Supplementary Table 2). Using data from 261 ERα$^+$ breast cancer patients, each assigned to a high- or low-genomic UPR grade, we observed reduced time to relapse for patients overexpressing the UPR signature (hazard ratio (HR) = 5.5, 95% CI: 3.1–9.8) (Supplementary Figures 9a and b). To evaluate the UPR signature in patients undergoing tamoxifen therapy, samples collected from 474 ERα$^+$ breast cancer patients, prior to starting 5-years of tamoxifen therapy, were assigned to low, medium, or high UPR risk groups. Increased prior expression of the UPR gene signature was tightly correlated with subsequent reduced time to recurrence (Figure 6b and d; Supplementary Figure 9c). Hazard ratios increased from 2.2 to 3.7 for the medium and high-risk groups, respectively, suggesting that recurrence risk is sensitive to levels of the UPR gene signature (Figure 6b). The UPR index provides prognostic information beyond current clinical covariates. In a cohort of 236 ERα$^+$ breast cancer patients, UPR overexpression was strongly predictive of reduced survival (HR 2.69, 95% CI: 1.3–5.6), over and above clinical covariates alone (tumor grade, node involvement, tumor size and ERα status) (Figures 6c and d; Supplementary Figure 9d). Thus, the UPR index is a powerful prognostic gene signature in ERα$^+$ breast cancer with predictive power to stratify patients into high and low risk groups.

DISCUSSION

In contrast to the well-studied “reactive mode” of UPR activation that occurs in response to endoplasmic reticulum stress, there are few studies of UPR activation that anticipates the future need for increased capacity to fold and sort proteins, and occurs in the absence of endoplasmic reticulum stress.[7] Anticipatory UPR activation is observed in B-cell differentiation where UPR activation in plasma cells precedes the massive production and secretion of immunoglobulins.[13, 14] Because the signals responsible for anticipatory activation of the UPR are largely unknown, it is poorly understood.

In the absence of cell stress or misfolded proteins, the mitogen, estrogen, acting via ERα, triggers anticipatory activation of the UPR in breast and ovarian cancer cells. In less than 2 minutes, E_2-ERα triggers PLCγ-mediated opening of EnR IP_3R calcium channels and release of Ca^{2+} into the cytosol. This increase in cytosol Ca^{2+} stimulates activation of all three arms of the UPR and is required for E_2-ERα-stimulated cell proliferation.

Anticipatory activation of the UPR by E_2-ERα enhances EnR protein folding capacity, and thereby primes cells to meet the higher protein folding and sorting demands that characterize the later growth phases of the cell cycle. The major EnR chaperone BiP, plays a central role in EnR homeostasis, protein processing, and UPR signaling. Since BiP knockdown stimulates UPR activation and promotes EnR stress-induced apoptosis,[10, 28] and cells

undergoing E_2-mediated apoptosis have lower levels of chaperones,[29] we assessed the consequences of abrogating the expansion of EnR protein-folding capacity by blocking anticipatory activation of the UPR. PLCγ, IP_3R or ATF6α knockdown blocked E_2-induction of BiP and inhibited E_2-ERα stimulated proliferation of T47D cells. While IP_3R knockdown nearly abolished E_2-ERα-stimulated Ca^{2+} release from the EnR, and this blocked UPR activation, it did not inhibit E_2-ERα-mediated gene expression. Thus, inhibition of E_2-ERα-stimulated UPR activation and chaperone induction is sufficient to inhibit E_2-ERα-stimulated cell proliferation. Using 2-APB and ryanodine together, or chelating intracellular calcium with BAPTA, completely abrogated the increase in intracellular calcium, and blocked E_2-ERα-regulated gene expression. Based on the inhibitor and knockdown data, we hypothesize that very small increases in intracellular calcium are sufficient to enable E_2-ERα-regulated gene expression and that somewhat larger increases in intracellular calcium are likely required for E_2-ERα activation of the UPR. E_2-ERα induces a substantial increase in intracellular calcium, which may promote coordination between the nucleus and endoplasmic reticulum, and couple activation of the E_2-ERα genomic program with UPR activation and expansion of the EnR protein-folding capacity.

We further validated the importance of this novel extranuclear pathway of E_2-ERα action using MCF-7 cells to assess how knockdown of each pathway component affects E_2-ERα-stimulated cell proliferation. PERK knockdown produced a 20% decline in E_2-ERα-stimulated cell proliferation. Although seemingly detrimental to promoting cell proliferation, PERK activation may be required to fully activate the ATF6α arm of the UPR.[30] Knockdown of XBP1 or ATF6α produced a 40% decline in E_2-ERα-stimulated cell proliferation. IP_3R knockdown produced an even larger reduction in E_2-ERα stimulated cell proliferation, while PLCγ knockdown had the largest effect. Thus, anticipatory activation of the UPR plays an important role in E_2-ERα dependent proliferation of cancer cells.

As expected,[1, 3] IDC tumor samples exhibited increased ERα expression and activation compared to normal breast epithelial tissue. Consistent with a role for the UPR in this proliferative phase of early tumor development, increased UPR expression and activation was observed in IDC tumor samples. This suggests that increased UPR expression occurs early in tumor development, long before detection, diagnosis, and the initiation of treatment.

Activation of the UPR by E_2-ERα exerts a long-term impact on the pathology of ERα positive breast cancer. Weak activation of the UPR by estrogen, or by tunicamcyin, elicits an adaptive response that protects cells from subsequent exposure to higher levels of cell stress. We explored whether the effects of E_2-ERα on the UPR correlated with clinical resistance to tamoxifen therapy. Increased UPR activation and elevated expression of UPR components were predictive of a poor response to tamoxifen-therapy, shorter time to recurrence, and decreased overall survival. If UPR expression promotes resistance to tamoxifen therapy, some UPR genes should exhibit differential regulation in our tamoxifen-sensitive MCF-7 tumors,[26] compared to their expression in the tamoxifen-resistance gene signature. Supporting this view, several genes encoding UPR components were E_2-downregulated in tamoxifen-sensitive MCF-7 tumors, but elevated in the human tumors expressing the tamoxifen-resistance gene signature (PERK, $p58^{IPK}$).

For ERα$^+$ breast cancers resistant to endocrine therapies, an important objective is development of more specific biomarkers that predict therapeutic response and identification of new therapeutic targets. The UPR is a new biomarker and therapeutic target in ERα$^+$ breast cancer; validated through mechanistic studies in culture, a mouse xenograft, and bioinformatics analysis of patient tumor samples. Anticipatory estrogen activation of the UPR is a novel extranuclear action of ERα, a previously undescribed early component of the estrogen-ERα cell proliferation program and a new paradigm by which estrogens may influence tumor development and resistance to therapy.

MATERIALS AND METHODS

Cell Culture and Reagents

Cell culture medium and conditions were previously described.[31–33] MCF-7, T47D, and T47D-kBluc cells were obtained from the ATCC. Drs. S. Kaufmann and K. Korach provided PEO4 cells and BG-1 cells, respectively. E_2, 4-OHT, U73122, 2-APB, and tunicamycin were from Sigma Aldrich. ICI 182,780 was from Tocris Biosciences and ryanodine was from Santa Cruz Biotechnology. Phospho-eIF2α (#3398), eIF2α (#5324), Phospho-PERK (#3179), PERK (#5683), and BiP (#3177) antibodies were from Cell Signaling. Pan-IP_3R (sc-28613), XBP1 (sc-7160), and ERα (sc-56836) antibodies were from Santa Cruz Biotechnology. Other antibodies used were ATF6α (Imgenex) and β-Actin (Sigma).

Cell Proliferation Assays

Cells proliferation assays were carried out as described.[31–33]

Protein Synthesis

Protein synthesis was evaluated by measuring incorporation of ^{35}S-Methionine into newly synthesized protein. Cells were incubated in 96 well plates for 20 minutes with 3 μCi of ^{35}S-methionine per well (PerkinElmer), lysed, and clarified by centrifugation. The appropriate volume, normalized to total protein, was spotted onto Whatman 540 filter paper discs and immersed in cold 10% TCA and washed in 5% TCA. Trapped protein was solubilized and filters counted.

Calcium Imaging

Cytoplasmic Ca^{2+} concentrations were measured using the calcium-sensitive dye, Fluo-4 AM.[34, 35] Cells were grown on 35 mm-fluorodish plates (World Precision Instruments) for two days prior to experiments. Cells were loaded with 5 μM Fluo-4 AM (Life Technologies) in buffer (140 mM NaCl, 4.7 mM KCl, 1.13 mM $MgCl_2$, 10 mM HEPES, 10 mM Glucose, pH = 7.4) for 30 minutes at 37° C. The cells were washed three times with buffer and incubated with either 2 mM or 0 mM $CaCl_2$ for 10 minutes. Images were captured for one minute to determine basal fluorescence intensity, and then the appropriate treatment was added. Measurements used a Zeiss LSM 700 confocal microscope with a Plan-Four 20X objective (N.A. = 0.8) and 488-nM laser excitation (7% power). Images were obtained through monitoring fluorescence emission at 525 nM, and analyzed with AxioVision and Zen software (Zeiss).

Luciferase Assays, qRT-PCR, and siRNA Transfections

Reporter gene assays and qRT-PCR were previously described.[31, 32] siRNA knockdowns were performed using DharmaFECT1 Transfection Reagent and 100 nM ON-TARGETplus non-targeting pool or SMARTpools for ERα (ESR1), PLCγ (PLCG1), PERK (EIF2AK3), ATF6α (ATF6), XBP1, or pan-IP3R (Dharmacon). The pan-IP_3R SmartPool consisted of three individual SmartPools, each at 33 nM, directed against each isoform of the IP_3R (ITPR1, ITPR2, and ITPR3).

MCF-7 Xenograft

Experiment were approved by the Institutional Animal Care Committee (IACUC) of the University of Illinois at Urbana-Champaign. The MCF-7 cell mouse xenograft model has been described previously.[26] Estrogen pellets (1 mg:19 mg estrogen:cholesterol) were implanted into 30 athymic female OVX mice at 7 weeks of age. Three days later, 1 million MCF-7 human breast cancer cells suspended in matrigel were subcutaneously injected into two sites on each flank, for a total of 4 tumors per mouse. When average tumor size reached 17.6 mm^2, E_2 pellets were removed and a lower dose of E_2 in sealed silastic tubing (1:31 estrogen:cholesterol, 3 mg total weight) was implanted. When average tumor size reached 23.5 mm^2, 15 mice retained E_2 silastic tubes (+E_2 group) and 15 mice received silastic tubes containing only cholesterol (−E_2 group). Tumors were measured every 4 days with a caliper. Tumor cross sectional area was calculated as (a/2)*(b/2)*3.14, where a and b were the measured diameters of each tumor. Upon termination of the experiments, mice were euthanized and tumors were excised.

Tumor Microarray Data Analysis

Analysis was performed using publically available tumors cohorts. ERα and UPR gene expression profiles of histologically normal breast epithelium (GSE20437)[36] were compared to IDC tumors from $ERα^+$ breast cancer patients (GSE20194). ERα and UPR correlation analysis was performed on 278 invasive ductal carcinoma samples (GSE20194).[37] A “UPR Gene Signature” was constructed to carry out risk prediction analysis. The UPR gene signature was evaluated for its ability to predict: (i) tumor relapse in 261 early-stage $ERα^+$ breast cancers (GSE6532),[37] (ii) tumor relapse in 474 $ERα^+$ patients receiving solely tamoxifen therapy for 5 years (GSE6532, GSE17705),[38, 39] and (iii) overall survival in a mixed-cohort of 236 breast cancer patients (GSE3494).[40] Microarray data analysis was performed using BRB ArrayTools (version 4.2.1) and R software version 2.13.2. Gene expression values from CEL files were normalized by use of the standard quantile normalization method.[41] Pearson correlation tests and Spearman log rank tests were used to determine gene expression correlation coefficients. Wald tests were used to test whether UPR genes were predictive of tumor recurrence and overall survival. Univariate and multivariate hazard ratios were estimated using Cox regression analysis. Covariates statistically significant in univariate analysis were further assessed in multivariate analysis. A patient was excluded from multivariate analysis, if data for one or more variables was missing. Risk prediction using the UPR gene signature was carried out using the supervised principle components method,[42] and visualized using Kaplan-Meier plots and compared using log-rank tests.

Statistical Analysis

Calcium measurements are reported as mean ± SE. All other data is reported as mean ± S.E.M. Two-tailed student's t-test used for comparisons between groups. One-way ANOVA followed by Fisher's LSD or Tukey's post hoc test used for multiple comparisons. $P < 0.05$ was considered significant.

Supplementary Material

Refer to Web version on PubMed Central for supplementary material.

Acknowledgments

We thank Mr. J. Hartman for assistance with xenografts, and Drs. S. Kaufmann and K. Korach for cell lines. Supported by NIH RO1DK 071909 (to D.S.) and Westcott and Carter predoctoral fellowships (to N.A.). Analyses were performed using BRB-ArrayTools, developed by Dr. Richard Simon and BRB-ArrayTools Development Team at the National Cancer Institute.

References

1. Korach KSDBJ. Estrogen receptors and human disease. J Clin Inv. 2006; 116:561–571.
2. Musgrove EA, Sutherland RL. Biological determinants of endocrine resistance in breast cancer. Nat Rev Cancer. 2009; 9:631–643. [PubMed: 19701242]
3. Yue W, Yager JD, Wang JP, Jupe ER, Santen RJ. Estrogen receptor-dependent and independent mechanisms of breast cancer carcinogenesis. Steroids. 2013; 78:161–170. [PubMed: 23178278]
4. (EBCTCG). EBCTCG. Effects of chemotherapy and hormonal therapy for early breast cancer on recurrence and 15-year survival: an overview of the randomised trials. Lancet. 2005; 365:1687–1717. [PubMed: 15894097]
5. Jensen EV, Jordan VC. The estrogen receptor: a model for molecular medicine. Clin Cancer Res. 2003; 9:1980–1989. [PubMed: 12796359]
6. Ron D, Walter P. Signal integration in the endoplasmic reticulum unfolded protein response. Nat Rev Mol Cell Biol. 2007; 8:519–529. [PubMed: 17565364]
7. Walter P, Ron D. The unfolded protein response: from stress pathway to homeostatic regulation. Science. 2012; 334:1081–1086. [PubMed: 22116877]
8. Ma Y, Hendershot LM. The role of the unfolded protein response in tumour development: friend or foe? Nat Rev Cancer. 2004; 4:966–977. [PubMed: 15573118]
9. Luo B, Lee AS. The critical roles of endoplasmic reticulum chaperones and unfolded protein response in tumorigenesis and anticancer therapies. Oncogene. 2013; 32:805–818. [PubMed: 22508478]
10. Dong D, Ni M, Li J, Xiong S, Ye W, Virrey JJ, et al. Critical role of the stress chaperone GRP78/BiP in tumor proliferation, survival, and tumor angiogenesis in transgene-induced mammary tumor development. Cancer Res. 2008; 68:498–505. [PubMed: 18199545]
11. Lee E, Nichols P, Spicer D, Groshen S, Yu MC, Lee AS. GRP78 as a novel predictor of responsiveness to chemotherapy in breast cancer. Cancer Res. 2006; 66:7849–7853. [PubMed: 16912156]
12. Fu Y, Li J, Lee AS. GRP78/BiP inhibits endoplasmic reticulum BIK and protects human breast cancer cells against estrogen starvation-induced apoptosis. Cancer Res. 2007; 67:3734–3740. [PubMed: 17440086]
13. Hu CC, Dougan SK, McGehee AM, Love JC, Ploegh HL. XBP-1 regulates signal transduction, transcription factors and bone marrow colonization in B cells. EMBO J. 2009; 28:1624–1636. [PubMed: 19407814]

14. van Anken E, Romijn EP, Maggioni C, Mezghrani A, Sitia R, Braakman I, et al. Sequential waves of functionally related proteins are expressed when B cells prepare for antibody secretion. Immunity. 2003; 18:243–253. [PubMed: 12594951]
15. Perou CM, Sorlie T, Eisen MB, van de Rijn M, Jeffrey SS, Rees CA, et al. Molecular portraits of human breast tumours. Nature. 2000; 406:747–752. [PubMed: 10963602]
16. Wang DY, Fulthorpe R, Liss SN, Edwards EA. Identification of estrogen-responsive genes by complementary deoxyribonucleic acid microarray and characterization of a novel early estrogen-induced gene: EEIG1. Mol Endocrinol. 2004; 18:402–411. [PubMed: 14605097]
17. Ding L, Yan J, Zhu J, Zhong H, Lu Q, Wang Z, et al. Ligand-independent activation of estrogen receptor alpha by XBP-1. Nucleic Acids Res. 2003; 31:5266–5274. [PubMed: 12954762]
18. Gomez BP, Riggins RB, Shajahan AN, Klimach U, Wang A, Crawford AC, et al. Human X-box binding protein-1 confers both estrogen independence and antiestrogen resistance in breast cancer cell lines. Faseb J. 2007; 21:4013–4027. [PubMed: 17660348]
19. Lee AH, Iwakoshi NN, Glimcher LH. XBP-1 regulates a subset of endoplasmic reticulum resident chaperone genes in the unfolded protein response. Mol Cell Biol. 2003; 23:7448–7459. [PubMed: 14559994]
20. Wu J, Rutkowski DT, Dubois M, Swathirajan J, Saunders T, Wang J, et al. ATF6alpha optimizes long-term endoplasmic reticulum function to protect cells from chronic stress. Dev Cell. 2007; 13:351–364. [PubMed: 17765679]
21. Okada T, Yoshida H, Akazawa R, Negishi M, Mori K. Distinct roles of activating transcription factor 6 (ATF6) and double-stranded RNA-activated protein kinase-like endoplasmic reticulum kinase (PERK) in transcription during the mammalian unfolded protein response. Biochem J. 2002; 366:585–594. [PubMed: 12014989]
22. Rutkowski DT, Arnold SM, Miller CN, Wu J, Li J, Gunnison KM, et al. Adaptation to ER stress is mediated by differential stabilities of pro-survival and pro-apoptotic mRNAs and proteins. PLoS Biol. 2006; 4:e374. [PubMed: 17090218]
23. Divekar SD, Storchan GB, Sperle K, Veselik DJ, Johnson E, Dakshanamurthy S, et al. The role of calcium in the activation of estrogen receptor-alpha. Cancer Res. 2011; 71:1658–1668. [PubMed: 21212417]
24. Frasor J, Danes JM, Komm B, Chang KC, Lyttle CR, Katzenellenbogen BS. Profiling of estrogen up- and down-regulated gene expression in human breast cancer cells: insights into gene networks and pathways underlying estrogenic control of proliferation and cell phenotype. Endocrinology. 2003; 144:4562–4574. [PubMed: 12959972]
25. Rae JM, Johnson MD, Scheys JO, Cordero KE, Larios JM, Lippman ME. GREB 1 is a critical regulator of hormone dependent breast cancer growth. Breast Cancer Res Treat. 2005; 92:141–149. [PubMed: 15986123]
26. Ju YH, Doerge DR, Allred KF, Allred CD, Helferich WG. Dietary genistein negates the inhibitory effect of tamoxifen on growth of estrogen-dependent human breast cancer (MCF-7) cells implanted in athymic mice. Cancer Res. 2002; 62:2474–2477. [PubMed: 11980635]
27. Rutkowski DT, Kaufman RJ. That which does not kill me makes me stronger: adapting to chronic ER stress. Trends Biochem Sci. 2007; 32:469–476. [PubMed: 17920280]
28. Rao RV, Peel A, Logvinova A, del Rio G, Hermel E, Yokota T, et al. Coupling endoplasmic reticulum stress to the cell death program: role of the ER chaperone GRP78. FEBS Lett. 2002; 514:122–128. [PubMed: 11943137]
29. Ariazi EA, Cunliffe HE, Lewis-Wambi JS, Slifker MJ, Willis AL, Ramos P, et al. Estrogen induces apoptosis in estrogen deprivation-resistant breast cancer through stress responses as identified by global gene expression across time. Proc Natl Acad Sci U S A. 2011; 108:18879–18886. [PubMed: 22011582]
30. Teske BF, Wek SA, Bunpo P, Cundiff JK, McClintick JN, Anthony TG, et al. The eIF2 kinase PERK and the integrated stress response facilitate activation of ATF6 during endoplasmic reticulum stress. Mol Biol Cell. 2011; 22:4390–4405. [PubMed: 21917591]
31. Andruska N, Mao C, Cherian M, Zhang C, Shapiro DJ. Evaluation of a luciferase-based reporter assay as a screen for inhibitors of estrogen-ERalpha-induced proliferation of breast cancer cells. J Biomol Screen. 2012; 17:921–932. [PubMed: 22498909]

32. Cherian MT, Wilson EM, Shapiro DJ. A competitive inhibitor that reduces recruitment of androgen receptor to androgen-responsive genes. J Biol Chem. 2012; 287:23368–23380. [PubMed: 22589544]

33. Kretzer NM, Cherian MT, Mao C, Aninye IO, Reynolds PD, Schiff R, et al. A noncompetitive small molecule inhibitor of estrogen-regulated gene expression and breast cancer cell growth that enhances proteasome-dependent degradation of estrogen receptor {alpha}. J Biol Chem. 2010; 285:41863–41873. [PubMed: 21041310]

34. Dong S, Teng Z, Lu FH, Zhao YJ, Li H, Ren H, et al. Post-conditioning protects cardiomyocytes from apoptosis via PKC (epsilon)-interacting with calcium-sensing receptors to inhibit endo (sarco) plasmic reticulum-mitochondria crosstalk. Mol Cell Biochem. 2010; 341:195–206. [PubMed: 20383739]

35. Spiller DG, Wood CD, Rand DA, White MR. Measurement of single-cell dynamics. Nature. 2010; 465:736–745. [PubMed: 20535203]

36. Graham K, de las Morenas A, Tripathi A, King C, Kavanah M, Mendez J, et al. Gene expression in histologically normal epithelium from breast cancer patients and from cancer-free prophylactic mastectomy patients shares a similar profile. Br J Cancer. 2010; 102:1284–1293. [PubMed: 20197764]

37. Shi L, Campbell G, Jones WD, Campagne F, Wen Z, Walker SJ, et al. The MicroArray Quality Control (MAQC)-II study of common practices for the development and validation of microarray-based predictive models. Nat Biotechnol. 2010; 28:827–838. [PubMed: 20676074]

38. Loi S, Haibe-Kains B, Desmedt C, Lallemand F, Tutt AM, Gillet C, et al. Definition of clinically distinct molecular subtypes in estrogen receptor-positive breast carcinomas through genomic grade. J Clin Oncol. 2007; 25:1239–1246. [PubMed: 17401012]

39. Symmans WF, Hatzis C, Sotiriou C, Andre F, Peintinger F, Regitnig P, et al. Genomic index of sensitivity to endocrine therapy for breast cancer. J Clin Oncol. 2010; 28:4111–4119. [PubMed: 20697068]

40. Miller LD, Smeds J, George J, Vega VB, Vergara L, Ploner A, et al. An expression signature for p53 status in human breast cancer predicts mutation status, transcriptional effects, and patient survival. Proc Natl Acad Sci U S A. 2005; 102:13550–13555. [PubMed: 16141321]

41. Bolstad BM, Irizarry RA, Astrand M, Speed TP. A comparison of normalization methods for high density oligonucleotide array data based on variance and bias. Bioinformatics. 2003; 19:185–193. [PubMed: 12538238]

42. Bair E, Tibshirani R. Semi-supervised methods to predict patient survival from gene expression data. PLoS Biol. 2004; 2:E108. [PubMed: 15094809]

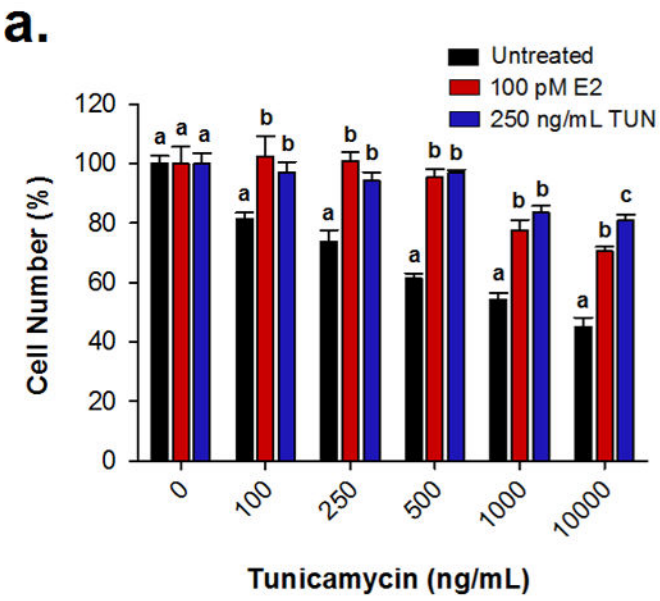

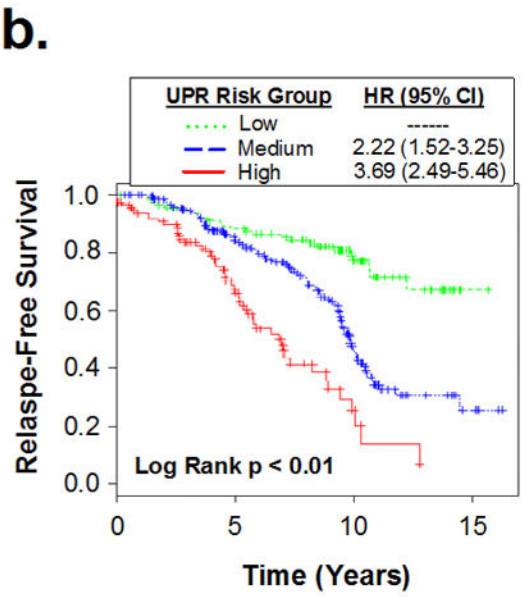

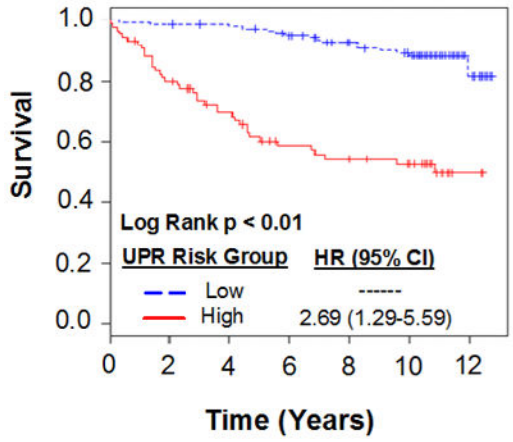

d.

	Univariate Analysis HR (95% CI)	p	Multivariate Analysis HR (95% CI)	p
Relapse-Free Survival				
Grade (3 vs. 2 + 1)	1.33 (0.79-2.26)	0.28	n.s.	n.s.
Tumor Size (>2 cm)	1.31 (0.90-1.90)	0.16	n.s.	n.s.
Node	1.54 (1.15-2.07)	0.00418	1.64 (1.22-2.21)	0.001
ERα*	1.30 (0.98-1.74)	0.074	n.s.	n.s.
ERα-Regulated Genes				
pS2*	1.27 (0.95-1.69)	0.107	n.s.	n.s.
PR*	0.81 (0.61-1.08)	0.142	n.s.	n.s.
XBP1*	1.79 (1.34-2.39)	9.0×10^{-5}	n.s.	n.s.
UPR Signature*	2.30 (1.71-3.09)	3.5×10^{-8}	2.44 (1.80-3.31)	1.0×10^{-8}
Overall Survival				
Grade (3 vs. 2 + 1)	2.02 (1.36-3.00)	0.003	1.30 (0.75-1.86)	0.382
Tumor Size (> 2 cm)	4.76 (2.51-9.03)	2×10^{-6}	2.90 (1.47-5.71)	0.002
Node (+/-)	4.04 (2.35-6.95)	4×10^{-7}	1.70 (0.87-3.31)	0.101
ERα	1.38 (0.81-2.35)	0.241	n.s.	n.s.
UPR Signature*	5.52 (3.10-9.82)	6×10^{-9}	2.69 (1.29-5.59)	0.007

Figure 1.

E_2-ERα activates the IRE1α and ATF6α arms of the UPR in breast and ovarian cancer cells, resulting in the induction of the major EnR chaperone, BiP. (**a**) qRT-PCR comparing the effect of estrogen (E2), ICI 182,780 (ICI) and 4-hydroxytamoxifen (4-OHT) on E_2-ERα induction of spliced-XBP1 (sp-XBP1) in ERα$^+$T47D breast cancer cells (n = 3; $-E_2$ set to 1). Different letters indicate a significant difference among groups ($p < 0.05$) using one-way ANOVA followed by Tukey's post hoc test. (**b**) qRT-PCR showing the effect of E_2-ERα on sp-XBP1 mRNA in ERα$^+$MCF-7 breast and PEO4 ovarian cancer cells (n = 3; $-E_2$ set to 1). P-values testing for significance between indicated group and -E2 group. (**c**) RNAi knockdown of ERα abolishes E_2-induction of sp-XBP1 in MCF-7 cells (n = 3). Cells treated with 100 nM non-coding control (NC) or ERα siRNA SmartPool, followed by treatment with E_2 for the indicated times (**d**) Western blot analysis showing full-length 90 kDa ATF6α (p90-ATF6α) and proteolytically cleaved 50 kDa ATF6α (p50-ATF6α) in E_2-treatedT47D

breast cancer cells. (**e**) RNAi knockdown of ATF6α blocks E_2-induction of BiP in T47D cells. Cells treated with 100 nM non-coding control (NC) or ATF6α siRNA SmartPool, followed by treatment with E_2 for 4 hours. (**f**) qRT-PCR showing the effect of E_2 on BiP mRNA in MCF-7 cells and in PEO4 ovarian cancer cells (n = 3; $-E_2$ set to 1). (**g**) Western blot analysis of BiP protein levels in MCF-7 cells treated with E_2. The fold-change in BiP protein levels is shown below each lane and was determined by quantifying BiP and β-Actin signals, and calculating the ratio of BiP/β-Actin (t=0, [$-E_2$], set to 1). (**h**) RNAi knockdown of ERα abolishes E_2-induction of BiP in MCF-7 cells (n = 3). Cells treated with 100 nM non-coding control (NC) or ERα siRNA SmartPool, followed by treatment with E_2 for the indicated times. Concentrations: E_2, 1 nM (a, d), 10 nM (b, c, e–h); ICI, 1 μM (a, d); 4-OHT, 1 μM (a). Data is mean ± S.E.M. * $p < 0.05$; ** $p < 0.01$; *** $p < 0.001$.

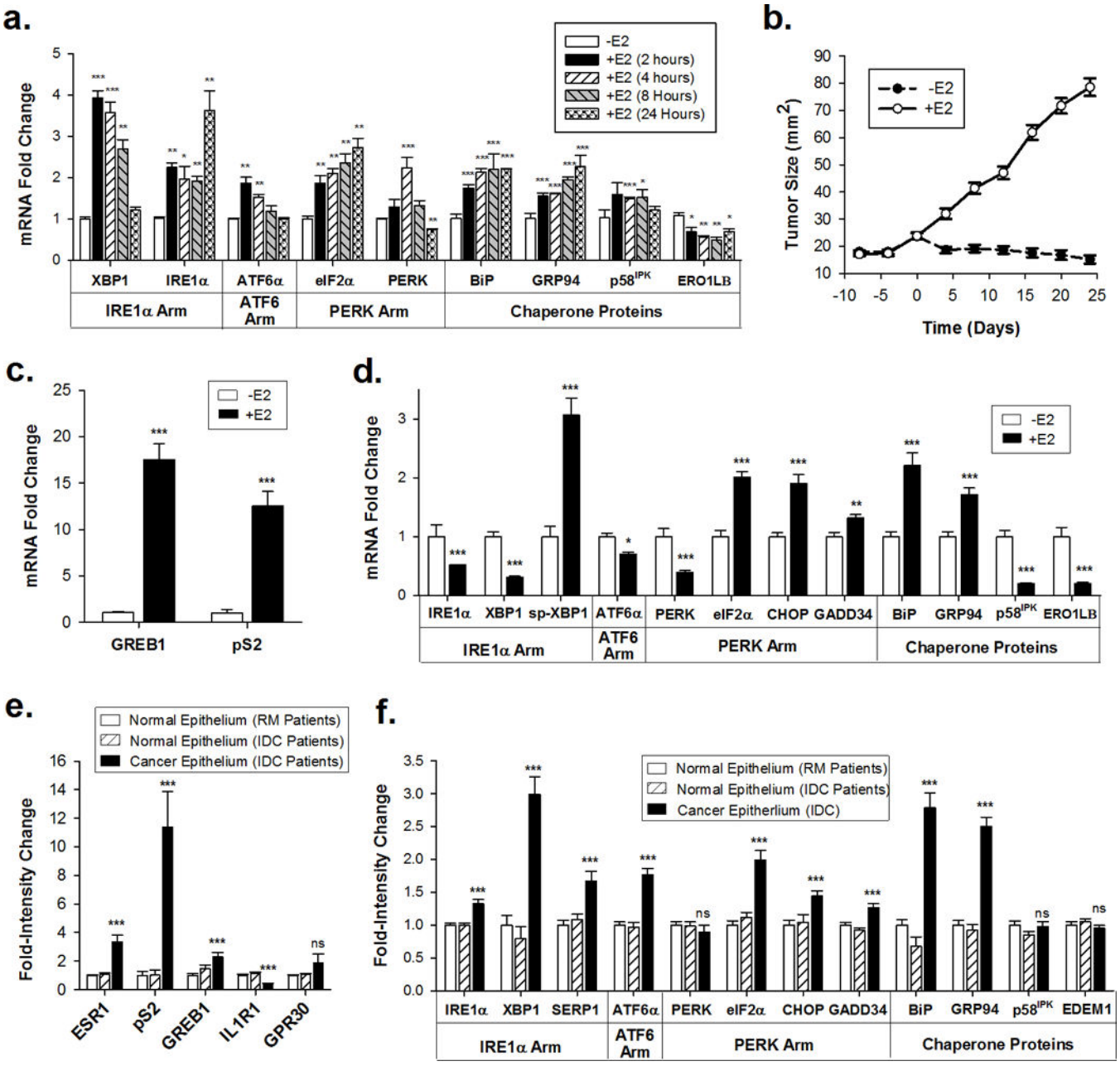

Figure 2.

E_2-ERα activates the PERK arm of the UPR. Western blot analysis showing (**a**) p-PERK and total PERK levels and (**b**) p-eIF2α levels and total eIF2α levels in $ERα^+$ T47D cells treated with ICI 182,780 (ICI) or a vehicle control for 2 hours, followed by treatment with 10 nM 17β-estradiol (E2) (n = 3). Numbers below each lane are the ratio of p-PERK/PERK or p-eIF2α/eIF2α normalized to the vehicle-treated control. (**c**) Protein synthesis in T47D breast cancer cells treated with ICI 182,780 (ICI) or a vehicle control for 2 hours, followed by treatment with 10 nM 17β-estradiol (E2) (n = 3). P-values testing for significance between indicated groups and -E2 samples. (**d**) PERK knockdown inhibits downstream phosphorylation of eIF2α in T47D cells. Cells treated with 100 nM non-coding control (NC)

or PERK siRNA SmartPool, followed by treatment with E_2 (+E2) or ethanol-vehicle (−E2) for 4 hours. (**e**) Western blot analysis of ATF4 following treatment of T47D cells with E_2, or the UPR activator tunicamycin (TUN). (**f**) qRT-pCR analysis of CHOP mRNA following treatment of T47D cells with E_2. Brackets denote pre-treatment with ICI for 2 hours. Concentrations: E_2, 1 nM (a–f); ICI, 1 μM (a, b, c); TUN, 10 μg/mL (e). Data is mean ± SEM. * $p<0.05$; ** $p<0.01$; *** $p< 0.001$; ns, not significant.

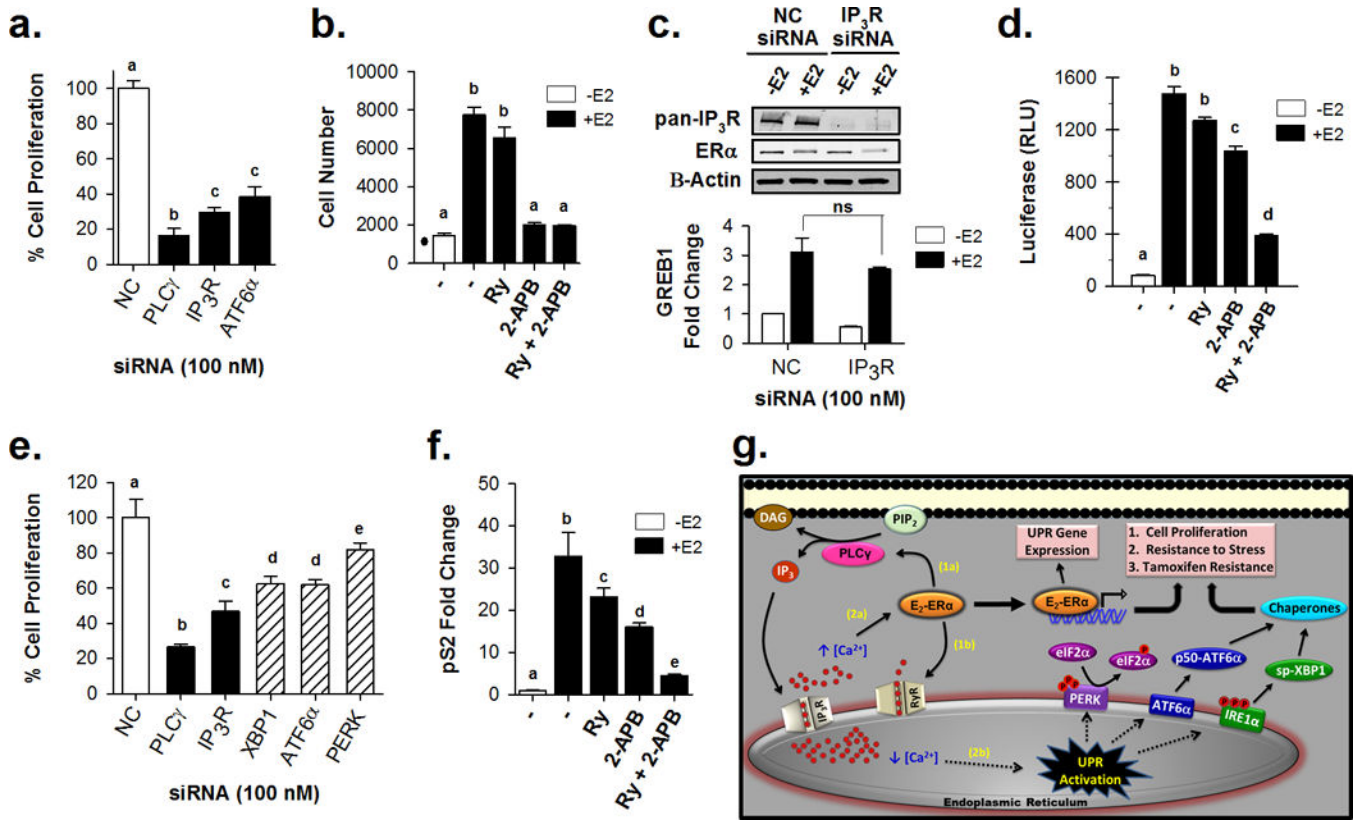

Figure 3.

Estrogen stimulates the release of calcium from the endoplasmic reticulum, and this calcium release is necessary for UPR activation. (**a**) Effects of 300 nM estrogen (E2) on cytosolic calcium levels in T47D breast cancer cells conditioned in the presence (2 mM $CaCl_2$) or absence (0 mM $CaCl_2$) of extracellular calcium, or cells pre-treated with 2-APB or ryanodine (Ry) for 30 minutes in the absence of extracellular calcium (0 mM $CaCl_2$). Visualization of intracellular Ca^{2+} using Fluo-4 AM. Colors from basal Ca^{2+} to highest Ca^{2+}: Blue, green, red, white. (**b**) Graph depicts quantitation of cytosolic calcium levels in T47D breast cancer cells treated with E_2 in the presence or absence of extracellular calcium, and in cells pre-treated with 2-APB or ryanodine (Ry) in the absence of extracellular calcium (n = 10 cells). E_2 was added at 60 sec, and fluorescence intensity prior to 60 sec was set to 1. (**c**) Western blot analysis of IP_3R and BiP protein levels following treatment of T47D cells with either 100 nM non-coding (NC) or IP_3R siRNA SmartPool, followed by treatment with E_2 (+E2) or ethanol-vehicle (−E2) for 4 hours. IP_3R smartpool contained equal amounts of three individual SmartPools directed against each isoform of IP_3R. (**d**) Quantitation of cytosolic Ca^{2+} levels in response to E_2, following treatment of T47D cells with 100 nM non-coding (NC) or IP_3R siRNA SmartPool (n = 10 cells) (**e**) Western blot analysis of PLCγ, BiP, and ATF6α protein levels after treatment of T47D cells with 100 nM non-coding (NC) or PLCγ siRNA SmartPool, followed by treatment with E_2 (+E2) or ethanol-vehicle (−E2) for 4 hours. (**f**) Quantitation of cytosolic Ca^{2+} levels in response to E_2, following treatment of T47D cells with 100 nM non-coding (NC) or PLCγ siRNA SmartPool. (**g**) Western blot analysis of ERα protein levels after treating T47D cells with

either 100 nM non-coding (NC) or ERα siRNA SmartPool, followed by treatment with E_2 (+E2) or ethanol-vehicle (−E2) for 4 hours. (**h**) Visualization and quantitation of cytosolic Ca^{2+} levels in response to E_2 after ERα knockdown in T47D cells. Concentrations: E_2, 300 nM (a, b, d, f, h), 1 nM (c, e, g); 2-APB, 200 μM (a, b); ryanodine, 200 μM (a, b). Graphical data is mean ± SE (n = 10).

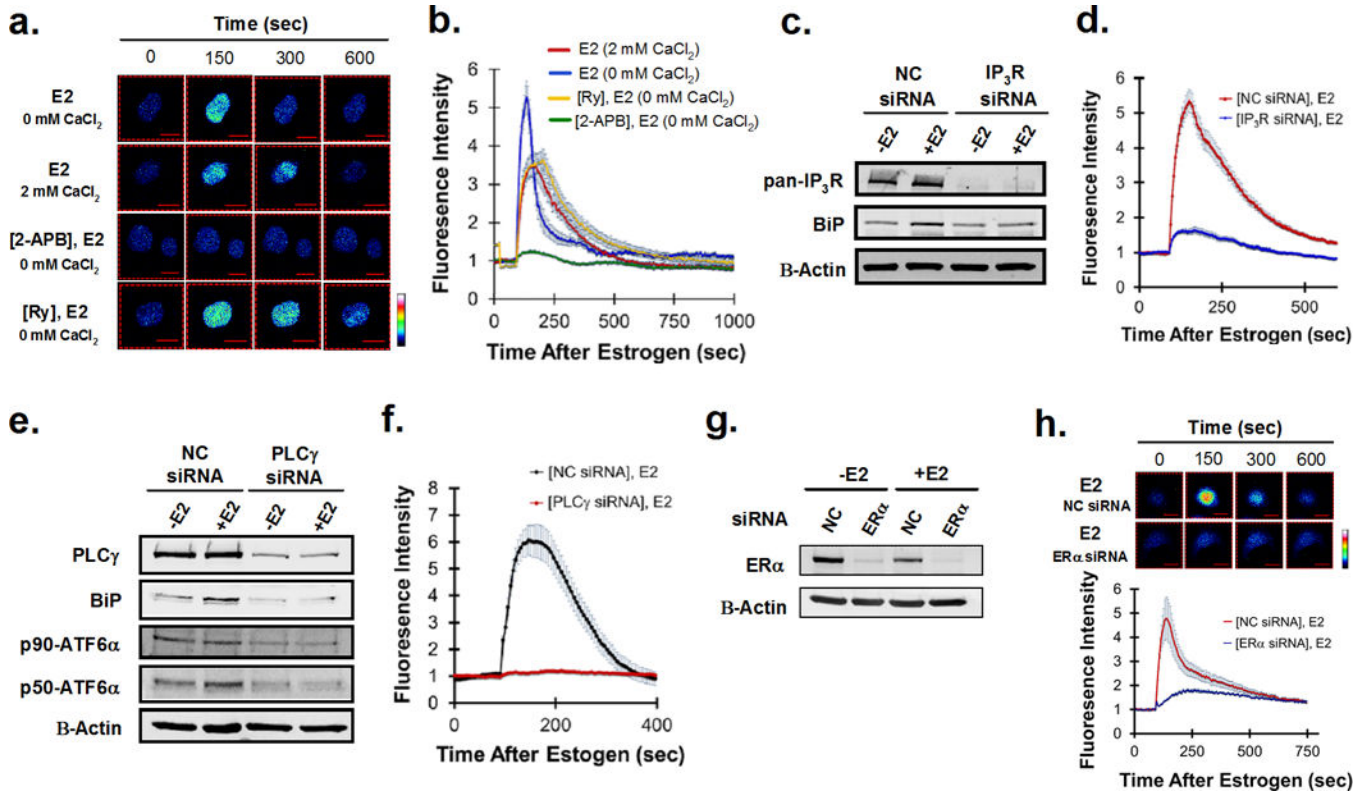

Figure 4.

E_2-ERα induced calcium release from the EnR into the cytosol is important for E_2-ERα mediated gene expression and E_2-ERα stimulated cell proliferation. (**a**) E_2-ERα stimulated proliferation of T47D breast cancer cells treated with 100 nM non-coding (NC), PLCγ, IP_3R, or ATF6α siRNA SmartPool (n = 6). Proliferation rates were normalized to cells treated with non-coding (NC) siRNA. (**b**) E_2-ERα stimulated proliferation of T47D breast cancer cells treated with ryanodine (Ry), 2-APB, or both inhibitors (Ry + 2-APB) for 4 days (n = 5). (**c**) qRT-PCR analysis of effects of IP_3R knockdown on E_2-ERα induction of GREB1 mRNA in T47D cells (n = 3). Western blot shows ERα protein levels after treatment of T47D cells with 100 nM non-coding (NC) or IP_3R siRNA SmartPool, followed by treatment with E_2 (+E2) or ethanol-vehicle (−E2) for 4 hours. (**d**) ERE-luciferase activity in kBluc-T47D breast cancer cells treated with E_2 and either ryanodine (Ry), 2-APB, or both inhibitors for 24-hours (Ry + 2-APB) (n = 4). (**e**) E_2-ERα stimulated proliferation of MCF-7 breast cancer cells treated 100 nM non-coding (NC), PLCγ, IP_3R, ATF6α, XBP1, or PERK siRNA SmartPool (n = 6). Proliferation rates were normalized to cells treated with non-coding (NC) siRNA. (**f**) qRT-PCR analysis of effects of ryanodine (Ry), 2-APB, or both inhibitors (Ry + 2-APB) on E_2-ERα induction of pS2 mRNA in MCF-7 cells (n = 3). (**g**) Model of E_2-ERα acting through the UPR to influence breast tumorigenesis.“•” denotes cell number at day 0. Concentrations: E_2, 100 pM (a–f); 2-APB, 200 μM (b, d, f); Ryanodine, 100 μM (b, d, f). Data is mean ± SEM. Different letters indicate a significant difference among groups ($p < 0.05$) using one-way ANOVA followed by Tukey’s post hoc test. ns, not significant.

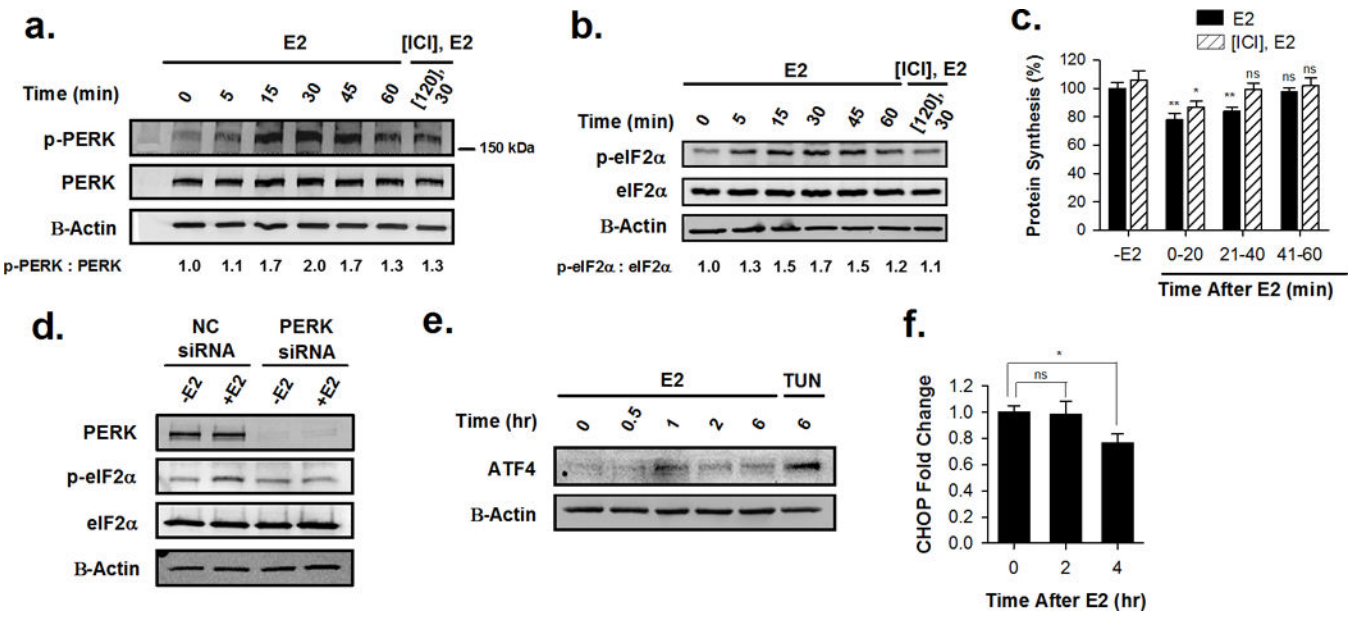

Figure 5.

E_2-ERα activity and UPR activity are correlated *in vivo*. (**a**) qRT-PCR analysis of levels of mRNAs for each arm of the UPR after treatment of MCF-7 cells with 10 nM E_2 for the indicated times (n = 3). (**b**) MCF-7 tumor growth in the presence or absence of estrogen in athymic mice. All mice were treated with estrogen to induce tumor formation. On "Day 0", E_2 in silastic tubes was replaced with silastic tubes containing only cholesterol in the $–E_2$ group (n = 15), while silastic tubes were retained in the $+E_2$ treatment group (n = 15). qRT-PCR analysis of (**c**) classical E_2-ERα regulated genes and (**d**) the UPR in mouse tumors collected after 24 days of exposure to estrogen (+E2) or vehicle-control (−E2) (n = 15). Relative mRNA levels of (**e**) classical E_2-ERα regulated genes and (**f**) the UPR pathway in patient samples of normal breast epithelium taken from patients undergoing reduction mammoplasty (RM) (n = 18), histologically normal breast epithelium taken from patients diagnosed with invasive ductal carcinoma (IDC) (n = 9), and carcinoma epithelium taken from IDC patients (n = 20). p-values represent comparisons to –E2 groups (a, c, d) or to histologically normal breast epithelium from patients who underwent reduction mammoplasty (e, f). Data is mean ± SEM. * P <0.05; ** P <0.01; ***P < 0.001; ns, not significant.

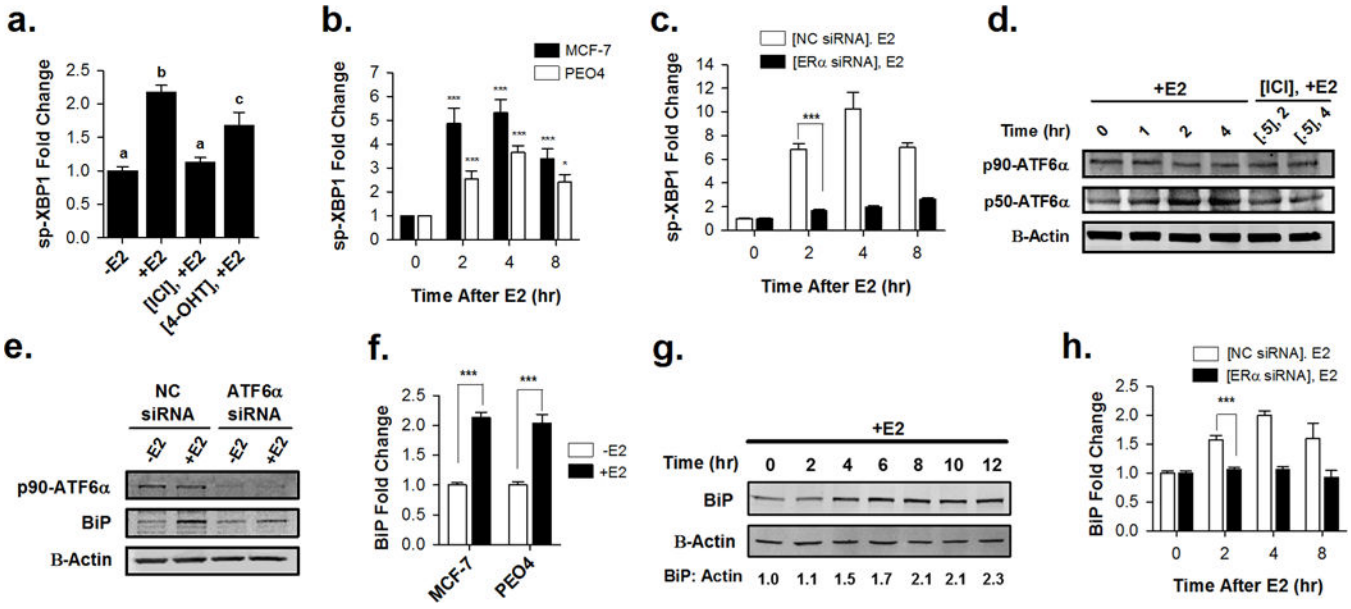

Figure 6.

Anticipatory activation of the UPR by estrogen protects cells from subsequent cell stress, and expression of the UPR gene signature predicts relapse-free and overall survival in ERα positive breast tumor cohorts. (**a**) Weak anticipatory activation of the UPR with estrogen or tunicamycin protects cells from subsequent UPR stress. T47D cells were maintained in 10% CD-FBS for 8 days and treated with either 250 ng/ml tunicamycin (TUN), 100 pM E_2, or ethanol/DMSO-vehicle (Untreated). E_2, TUN, or the vehicle control were removed from medium, and cells were harvested in 10% CD-calf serum and treated with the indicated concentrations of tunicamycin. Data is mean ± SEM (n = 6). Different letters indicate a significant difference among groups ($p < 0.05$) using one-way ANOVA followed by Fisher's LSD post hoc test. (**b**) Relapse-free survival as a function of the UPR gene signature for patients with $ERα^+$ breast cancer who subsequently received tamoxifen alone for 5 years. Interquartile range used to assign tumors to risk groups, representing UPR activity from high to low. Hazard ratios are between low and medium and low and high UPR groups (n = 474). (**c**) Overall survival as a function of the UPR signature and clinical covariates (node status, tumor grade, ERα-status, tumor size). p-value is testing for significance between the combined model (UPR gene signature and clinical covariates) versus the covariates only model (multivariate analysis) (n = 236). (**d**) Univariate and multivariate Cox regression analysis of the UPR signature, clinical covariates, and classical estrogen-induced genes for time to recurrence and survival (n.s., not significant). Median used to classify tumors into high and low risk groups.